16 June 2000

ELSEVIER

Chemical Physics Letters 323 (2000) 312–322

CHEMICAL PHYSICS LETTERS

www.elsevier.nl/locate/cplett

Femtosecond relaxation of photoexcited *para*-nitroaniline: solvation, charge transfer, internal conversion and cooling

S.A. Kovalenko, R. Schanz, V.M. Farztdinov, H. Hennig, N.P. Ernsting *

Institut für Physikalische und Theoretische Chemie, Humboldt Universität zu Berlin, Bunsenstr. 1, D-10117 Berlin, Germany

Received 11 January 2000; in final form 4 April 2000

Abstract

The ultrafast relaxation of *p*-nitroaniline (PNA) in water and acetonitrile is studied experimentally and theoretically. Transient absorption spectra are measured by the pump–supercontinuum probe technique (PSCP) after 50 fs excitation at 400 nm. The relaxation includes several stages with distinct time scales: solvation, intramolecular charge transfer (CT), internal conversion and cooling. The spectral evolution before 100 fs reflects mainly solvation with dynamic Stokes shift of 3500 cm^{-1} in acetonitrile and 4000 cm^{-1} in water. CT and internal conversion are governed by twisting of the $-NO_2$ group and proceed in water with 120 and 250 fs, respectively. A hot ground state upon internal conversion is characterized by an initial temperature of 1400 K. The subsequent solute–solvent energy transfer is characterized by exponential behavior between 1 and 3 ps and by a nonexponential decay at longer delays, the solute cooling time lies in the range 0.85–1.3 ps.

1. Introduction

Para-nitroaniline (PNA) is one of the simplest organic molecules with strong solvatochromic [1–3] and nonlinear optical properties [4–7]. For decades these and other photochemical features of PNA have been the subject of extensive experimental [1–4,8–10] and theoretical [1,5–7,11–14] investigations. The following view emerges from these studies. The ground state of PNA has a dipole moment $\mu_g \approx 6$ D (in dioxane [15]). Upon $\pi\pi^*$ photo-excitation, electron transfer from $-NH_2$ to $-NO_2$ increases the dipole moment up to $\mu_e \approx 14$ D in the excited state [8,15]. This photo-induced charge transfer is the reason for a pronounced solvatochromic red shift of the absorption band, by 5300 cm^{-1}, when going from nonpolar cyclohexane to highly polar dimethylsulfoxide [2]. Fluorescence from PNA has never been observed under normal conditions but could be measured at low temperatures in polar solvents [3]. This suggests very fast thermally activated processes in the excited electronic state such as intersystem crossing or internal conversion.

Keiding et al. [10] have recently undertaken a sub-picosecond transient absorption study of PNA in water and dioxane. They found that the excited-state relaxation is extremely fast (< 0.3 ps) and dominated by internal conversion in both solvents. However, this estimate was obtained at the limit of the experimental time resolution (0.3 ps). Thus to expose the earliest evolution, new experiments with better time resolution are needed.

* Corresponding author. Fax: +49-30-20932365

0009-2614/00/$ - see front matter
PII: S0009-2614(00)00432-2

In this Letter, we report preliminary results about the photophysics of PNA. Transient absorption spectra in acetonitrile and water have been measured by the pump–supercontinuum probe (PSCP) technique [16,17] in a range 300–700 nm with 30 fs resolution, allowing observation of the complete spectral evolution. We observe for the first time transient stimulated emission from PNA. Early spectral changes reflect solvation and intramolecular rearrangements in the solute which are followed by internal conversion and cooling. Our interpretation of the spectral changes is guided by semiempirical (SAM1) calculations of PNA in solution with variable twisting and wagging angles of the $-NO_2$ and $-NH_2$ groups. Results from this modeling are in excellent agreement with the experiment. In particular, our calculations predict the key role of $-NO_2$ twisting in intramolecular charge transfer (CT) and for initiating internal conversion.

We also examine the cooling of hot solute molecules by the solvent as is reflected in the transient spectra. There have already been a number of experimental and theoretical studies in this field [18–22]. Our results show that the energy transfer from highly polar PNA to polar surrounding proceeds with a characteristic time of 1 ps that is much faster than in the case of nonpolar or weakly polar solutes.

2. Experimental

The optical scheme for the pump–supercontinuum probe experiment has been described in detail elsewhere [16]. Basic pulses of 40 fs, 100 μJ, at 1 kHz repetition rate, centred at 800 nm, are derived from a standard Ti:Sa oscillator–amplifier system [23]. After frequency doubling with a 0.2 mm BBO crystal, the pulses are split in two parts. The first is used as a pump with an energy of 1 μJ and a spot size of 200 μm on the sample. The second (10–12 μJ) is focused into a 2 mm calcium fluoride plate to generate a supercontinuum probe which is used in the spectral range 295–709 nm. The pump and probe beam are synchronously chopped at 30 and 60 Hz, respectively, every second probe pulse being used for base line measurements (without pumping). The probe beam has a diameter of 100 μm on the sample and intersects the pump beam at 6°. The sample net thickness is 0.2 mm and the fused silica windows are 0.16 mm thick. The optical density of PNA solution is 0.6 at the absorption maximum which corresponds to a concentration of 2×10^{-3} mol/l. The solution is flown out of the interaction region after each laser shot. After interaction with the sample, the supercontinuum is dispersed by a polychromator and registered on a photodiode array (512 pixels) with a spectral resolution of 1.5 nm. A part of the probe is split off before interaction and is dispersed and registered separately for reference. Typically 200 shots are averaged to give the wavelength dependent differential optical density $\Delta OD(t, \lambda)$ at every time step of 3.33 fs for a short scan of 1 ps, or at every step of 20 fs for a long scan of 12 ps.

Stationary absorption spectra were measured with a Shimadzu spectrophotometer. PNA (with melting point at 148°C) was used without further purification. All measurements were performed at 22°C.

3. Experimental results

3.1. Steady-state absorption spectra

Stationary absorption spectra of PNA in four solvents – cyclohexane, acetonitrile, water and dimethylsulfoxide – are shown in Fig. 1. When comparing cyclohexane to acetonitrile solutions, one

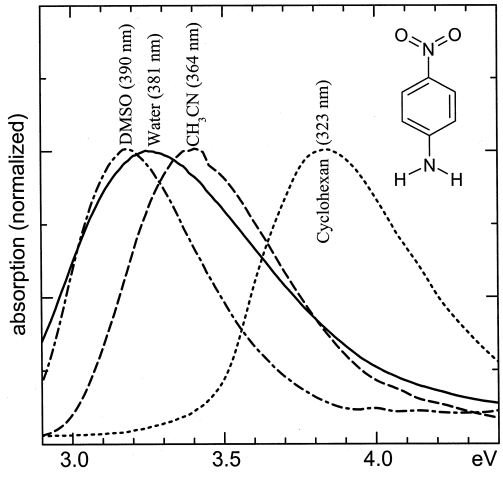

Fig. 1. Stationary absorption spectra of PNA in cyclohexane, acetonitrile, water and dimethylsulfoxide. Their spectral widths Γ (FWHM) in cm^{-1} in the same order: 4930, 4850, 6270 and 4130.

observes a red shift of the absorption band by 3500 cm^{-1} which is ascribed to solvation effects [2,24]. At the same time the width Γ of the band (FWHM) changes from 4930 to 4850 cm^{-1}, i.e. it *decreases* by going from a nonpolar to highly polar solvent. This trend is confirmed for dimethylsulfoxide in which $\Gamma = 4140$ cm^{-1}. Although water with $\Gamma =$ 6300 cm^{-1} is out of this trend (due to extra-broadening from hydrogen bonding) we consider the observed behavior – an increase of the band shift with decrease of the width – to be characteristic for PNA. This dependence is unusual and poses a question concerning the nature of spectral broadening in PNA.

3.2. Transient spectra

Transient absorption spectra measured in acetonitrile and water are shown in Fig. 2a,b and in Fig. 2c,d, respectively. Positive induced optical density ΔOD corresponds to excited-state absorption (ESA) while negative signal indicates bleach or stimulated emission (SE). The bleach band is peaked close to the pump wavelength near 400 nm, ESA is pronounced in the spectral region 300–350 nm, and stimulated emission is recognized in a range from 430 to 700 nm.

At early time, before 100 fs (frames a and c), major spectral evolution occurs for stimulated emission which shifts to the red. The time scale of this shift is less than 100 fs, i.e. consistent with solvation in water [25] and acetonitrile [26,27]. Thus the early evolution may be interpreted as reflecting mainly solvation processes.

For longer delays, between 100 fs and 1 ps (frames b and d), the ESA and SE band decay *simultaneously* indicating internal conversion to the ground

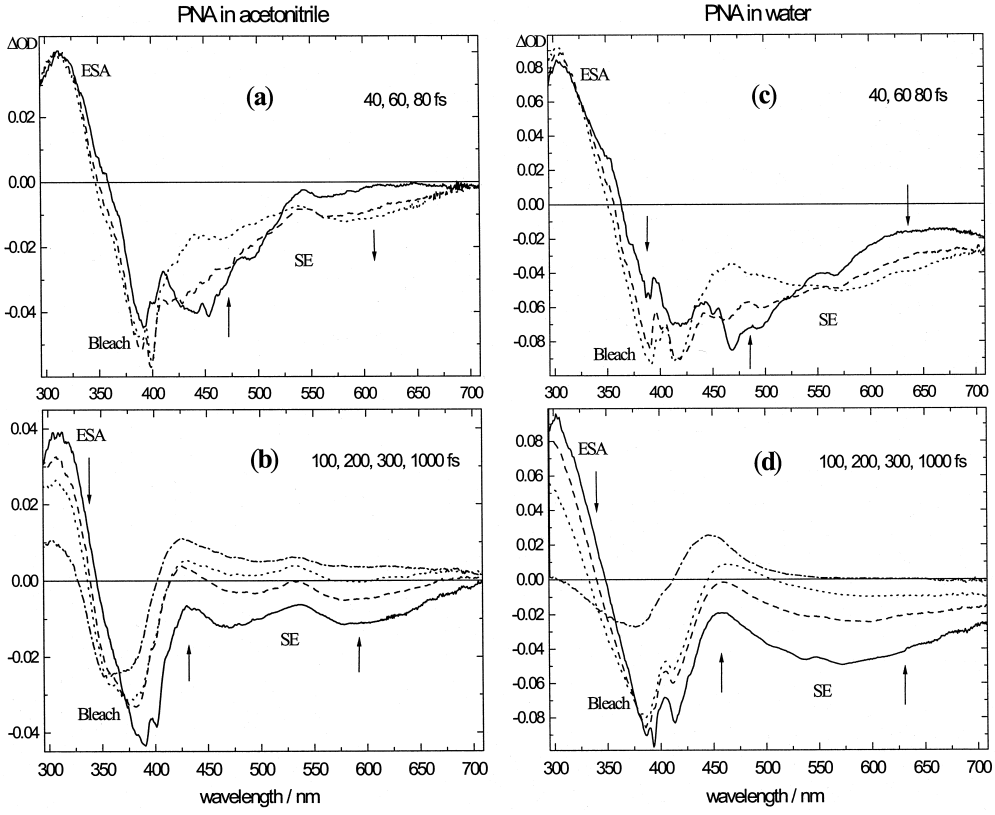

Fig. 2. Transient absorption spectra of PNA in acetonitrile (a and b) and in water (c and d). Spectra (a) and (c) are given at 40, 60 an 80 fs delays while (b) and (d) are at 100, 200, 300 and 1000 fs. Arrows indicate the evolution of the signal. ESA, excited-state absorption; SE, stimulated emission; pump wavelength at 400 nm.

electronic state. The characteristic time of internal conversion τ_{ic}, measured from the decay of ESA, is 250 fs in water and 400 fs in acetonitrile.

Lastly, Fig. 3a shows transient spectra of PNA in water measured from 1 to 10 ps. We assign these spectra to hot ground-state absorption overlapped with the bleach band (see Section 7). The true hot absorption spectra are obtained after bleach subtraction. When doing this we assume that the bleach band reproduces the stationary absorption spectrum of water in Fig. 1. The amplitude of bleach is adjusted to be around 0.1 as is directly seen from the transient spectrum at 100 fs (Fig. 2d). The resulting hot ground-state spectra are displayed in Fig. 3b for the same delays as the differential spectra in Fig. 3a.

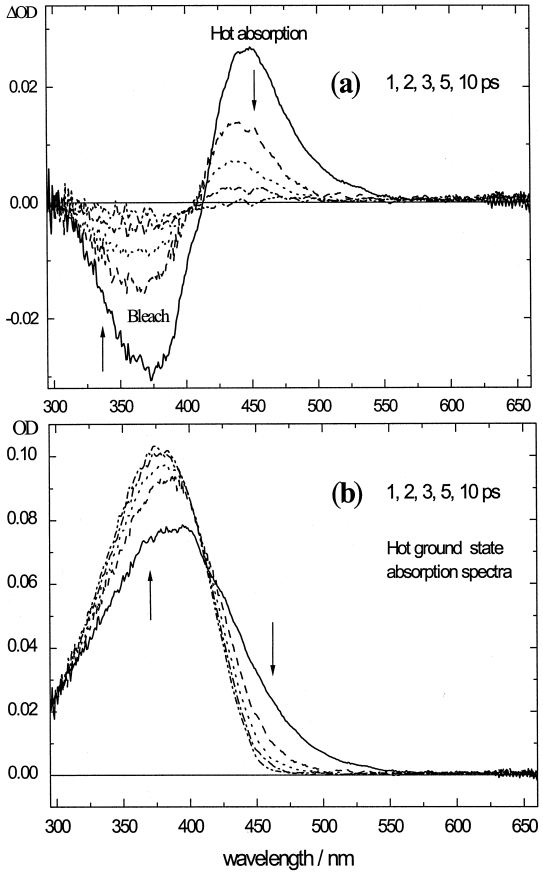

Fig. 3. (a) Transient absorption spectra of PNA in water at 1, 2, 3, 5, 10 ps; the signal decreases with time as indicated by arrows. (b) Hot ground-state absorption spectra for the same delays reconstructed from the spectra in frame (a) by bleach subtraction (see text).

For further analysis we introduce a band integral

$$\mathrm{BI}(t,\Delta\lambda)=\int_{\Delta\lambda}\Delta\mathrm{OD}(t,\lambda)\frac{\mathrm{d}\lambda}{\lambda} \qquad (1)$$

where $\Delta\lambda$ is the wavelength range over which the integral is taken. This quantity is extremely useful in transient absorption experiments with broad coverage such that it allows to monitor the full spectral evolution. The integral calculated over an *entire* band is insensitive to the spectral shift of the band. It reflects population dynamics if oscillator strengths of optical transitions do not change [24]. Alternatively for a constant population of the contributing electronic states, a change of the band integral signals changes in oscillator strengths for optical transitions from these states. Even for overlapping ESA and bleach bands or overlapping ESA and SE, the appropriate band integral provides useful information. In this case it remains to be proportional to the excited-state population and to *a difference* in oscillator strengths. Fig. 4a shows the evolution of two band integrals for PNA in water, calculated for the full spectral range 295–709 nm (dashed line) and for the red part of the spectrum, 430–709 nm (solid line). We will discuss these integrals in Sections 6 and 7.

We examine now in more detail the spectral evolution at early time. Let us start with acetonitrile (Fig. 2a,b). At 40 fs the stimulated emission band has its maximum (i.e. of negative ΔOD) at 440 nm. With increasing time the SE around 440 nm decreases while it increases at 600 nm (Fig. 2a). After 100 fs (Fig. 2b), two distinct maxima of the SE band are observed: the first around 470 nm and the second at 580 nm. When one keeps solvation as the only cause for spectral changes, a hump between two maxima must be assigned to excited-state absorption. Similarly, another small hump in the bleach region, at 400 nm, is also due to ESA. With this treatment, the true maximum for SE, say at 100 fs and later, is overlapped with ESA and should be located around 520 nm. This gives a maximum estimate for the dynamic Stokes shift $\Delta\nu_{solv}\approx 3500\ \mathrm{cm}^{-1}$.

Alternatively one may assume that the two maxima of SE correspond to different conformations of PNA in the excited state. Similarly, a hump at 400

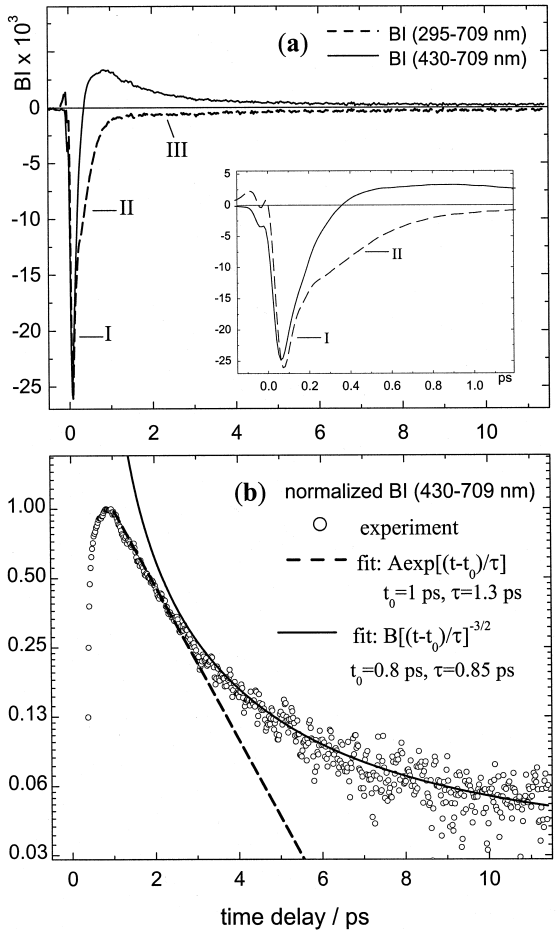

Fig. 4. (a) Band integral (BI) calculated with Eq. (1) for the range 295–709 nm (dashed line) and for the range 430–709 nm (solid line). Early evolution is shown as insert. Regions I, II, III are discussed in the text. (b) Normalized BI for 430–709 nm: circles, experiment; dashed line, 1 exponential fit, solid line, power fit.

nm may correspond to two different conformations in the ground state. Then the early spectral evolution, between 40 and 80 fs, reflects two simultaneous processes: solvation of the 'locally' excited molecular conformation, seen as a shift of the first SE band; and ultrafast intramolecular rearrangement which results in appearance of the second SE band around 580 nm. In this case a minimum estimate for the dynamic Stokes shift $\Delta\nu_{\mathrm{solv}}$, evaluated for the first band at later time (490 nm) is 2300 cm^{-1}.

The spectral evolution in water (Fig. 2c,d) is similar to that in acetonitrile, only the hump at 550 nm in the SE region is now less pronounced. Again two treatments are possible. For example, washing out the spectral hump at 400 nm in the bleach/ESA region (Fig. 2d) may be explained by a decrease of ESA due to internal conversion or it may be assigned to conformational relaxation in the ground state. Since the SE band is very broad, the dynamic Stokes shift (from 470 to 580 nm) can be evaluated only within the 'pure solvation' model giving $\Delta\nu_{\mathrm{solv}} =$ 4000 cm^{-1}.

4. Solvatochromic and dynamic Stokes shift in a continuum theory of solvation

Before we turn to semiempirical calculations, consider the relation between the dynamic shift $\Delta\nu_{\mathrm{solv}}$ of the SE band in a given solvent and the solvatochromic shift θ_{t} of the stationary absorption band between different solvents. In the dielectric continuum theory [24], assuming a solute to be a point dipole, we have

$$\Delta\nu_{\mathrm{solv}} = (2/hca^3)(\mu_{\mathrm{e}} - \mu_{\mathrm{g}})^2 f(\varepsilon,n) \qquad (2)$$

$$\Delta\nu_{\mathrm{abs}} \approx (2/hca^3)\mu_{\mathrm{g}}(\mu_{\mathrm{e}} - \mu_{\mathrm{g}})\,\Delta f(\varepsilon,n) \qquad (3)$$

Here a is the Onsager cavity radius and $f = (\varepsilon - 1)/(\varepsilon + 2) - (n^2 - 1)/(n^2 + 2)$ is a measure of solvent polarity, ε and n being the dielectric constant and refractive index. Let us compare these shifts when going from cyclochexane to acetonitrile (Fig. 1). In this case $\Delta f = f$, $\Delta\nu_{\mathrm{abs}} = 3500$ cm^{-1}, and (2) and (3) result in

$$\Delta\nu_{\mathrm{solv}} = \Delta\nu_{\mathrm{abs}} \cdot (\mu_{\mathrm{e}}/\mu_{\mathrm{g}} - 1) \qquad (4)$$

With $\mu_{\mathrm{g}} = 6$ D and $\mu_{\mathrm{e}} = 14$ D [8,15,28], one calculates an expected dynamic Stokes shift in acetonitrile $\Delta\nu_{\mathrm{solv}} = 4670$ cm^{-1}. This value exceeds both experimental estimates for the Stokes shift obtained above. However, because of better agreement with the estimate of 3500 cm^{-1} for the shift, it supports to some extent 'pure solvation' assignment of the early spectral evolution.

Another important quantity related to the dynamic shift $\Delta\nu_{\mathrm{solv}}$ is the width of absorption spectra associated with solvation [26]

$$\Gamma_{\mathrm{solv}} = 2.355\sqrt{\Delta\nu_{\mathrm{solv}} \cdot kT} \qquad (5)$$

In acetonitrile at room temperature we observed $\Delta\nu_{solv} = 3500\ cm^{-1}$ and obtain $\Gamma_{solv} = 1970\ cm^{-1}$. Now assume that the full spectral width can be expressed as $\Gamma = \sqrt{\Gamma_{solv}^2 + \Gamma_{intr}^2}$ where Γ_{intr} denotes intramolecular contributions. Since $\Gamma = 4850\ cm^{-1}$ from PNA absorption in acetonitrile, one obtains $\Gamma_{intr} = 4430\ cm^{-1}$. In turn Γ_{intr} contains broadening from the vibronic manifold of the electronically excited state(s) and that kind of broadening which may be called conformational broadening, when the electronic transition energy depends on the molecular geometry of the ground state. As will be shown in the next section, the latter contribution is large for PNA. Conformational effects may explain narrowing of the absorption band when going from nonpolar to polar solvents by a stabilization of an optimal molecular configuration.

5. Semiempirical calculations

SAM1 calculations (AMPAC 6.02) were performed on the PNA molecule imbedded in highly polar solvents (details are reported in Ref. [29]). Solvent effects are taken into account with the conductor-like screening model (COSMO) [30]. In this model, acetonitrile and water are nearly indistinguishable because specific solvation effects in water are not considered. Molecular properties of PNA are calculated depending on the twisting angle ϕ_t of the $-NO_2$ group and on the wagging angle ϕ_w of the $-NH_2$ group. Among the coordinates examined, these two angles are found to constitute the reaction coordinates for relaxation of PNA after photo-excitation.

Calculations are performed both for the ground state g and excited state e of PNA. They consist of closed shell (for e, open shell) self-consistent field calculations followed by configuration interaction. Results for the heat of formation H, static dipole moment μ, energy of electronic transitions E and oscillator strength f are collected in Table 1 and in Fig. 5. Table 1 contains values for the fully relaxed molecular geometry, and Fig. 5 shows their dependence on ϕ_t or ϕ_w while all other coordinates are allowed to relax.

When presenting results on the excited electronic state for given angle ϕ_t (or ϕ_w) we distinguish between *relaxed* and *nonrelaxed* nuclear configurations. The relaxed configuration corresponds, as usual, to the energy minimum – with respect to the remaining molecular coordinates and solvation – of the excited electronic state. Properties for the nonrelaxed configuration are calculated at the relaxed ground-state geometry for the given angle, but with solvation in the excited state. Nonrelaxed values are marked by a superscript ($'$).

5.1. Ground state properties

PNA in the ground state is nearly flat. A global minimum for the ground-state heat of formation H_g is found when $-NO_2$ is coplanar with the benzene ring ($\phi_t = 0°$) and $-NH_2$ is wagged ($\phi_w = 20°$) but not twisted. A lowest vibrational frequency of $\approx 20\ cm^{-1}$ is calculated for twisting of $-NO_2$. The potential energy in this direction is almost flat and $-NO_2$ can rotate nearly freely (Fig. 5a). The $-NH_2$ movement at room temperature is mainly wagging (Fig. 5b) with frequency of $360\ cm^{-1}$. Optical absorption corresponds to the $S_1 \leftarrow S_0$ transition; the calculated transition energy $E_{ge} = 3.8$ eV and oscillator strength $f_{ge} = 0.31$ at the global minimum are in reasonable agreement with experiment (3.4 eV and 0.32 [31]). E_{ge} depends strongly on ϕ_t and ϕ_w as is also shown

Table 1
Heat of formation H (relative to the ground state), dipole moment μ, transition energy E, oscillator strength f for the relaxed ground g and excited e state; m, n, higher excited states; ϕ_t and ϕ_w, equilibrium twisting and wagging angle of $-NO_2$ and $-NH_2$, respectively

	H (kcal/mol)	μ (D)	E (eV)	f	ϕ_t (NO_2) (degrees)	ϕ_w (NH_2) (degrees)
Ground g	0	8.8	$E_{ge} = 3.84$	$f_{ge} = 0.31$	0	21.5
Excited e	34.8	15.7	$E_{eg} = 0.0$	$f_{eg} = 0.0$	75	0
			$E_{em} = 2.4$	$f_{em} = 0.0$		
			$E_{en} = 4.7$	$f_{en} = 0.2$		

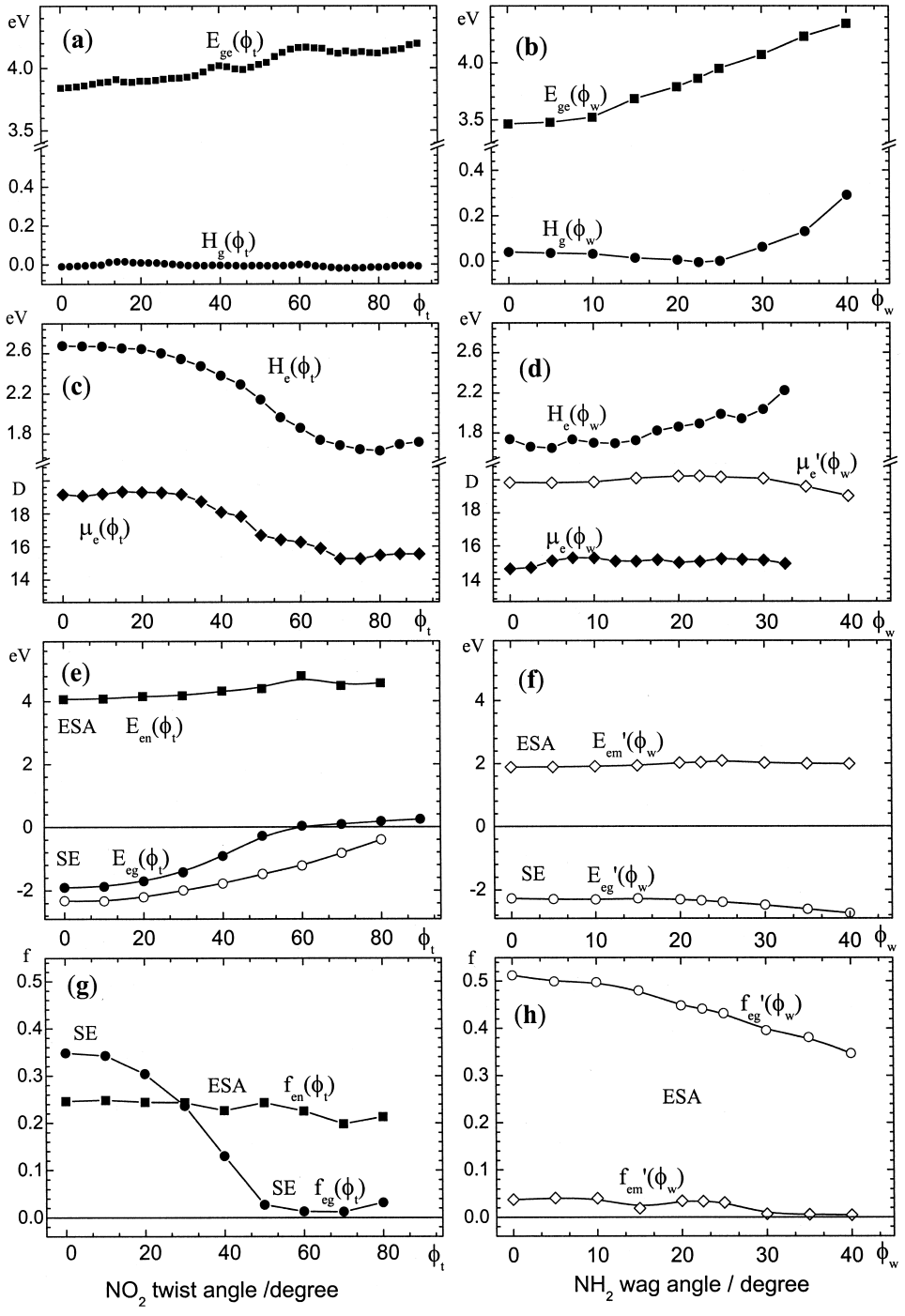

Fig. 5. Results of semiempirical calculations on PNA in water. Heat formation H, transition energy E, static dipole moment μ, and oscillator strength f are shown as functions of twisting angle θ_t of $-NO_2$ and of wagging angle θ_w of $-NH_2$. Subscripts g and e refer to the ground and excited state, m and n to higher electronic states. Solid symbols refer to relaxed and open symbols to nonrelaxed configurations (see text). Nonrelaxed parameters are marked by a superscript ($'$). ESA, excited-state absorption; SE, stimulated emission.

in Fig. 5a,b. The oscillator strength $f_{ge}(\phi_t, \phi_w)$ (not shown) decreases with an increase of both angles but stays > 0.16 for ϕ_t, $\phi_w < 40°$. Taken together with the thermal distributions of ϕ_t and ϕ_w in the ground state, we deduce a conformational broadening of the optical absorption band of 0.5 eV (≈ 4000 cm^{-1}). Conformational broadening should therefore dominate the intramolecular bandwidth $\Gamma_{intr} = 4430$ cm^{-1} which was estimated in Section 4.

5.2. Excited state properties

After photo-excitation the PNA molecule acquires a geometry which differs considerably from that in the ground state. Now a minimum for the heat of formation H_e is found when $-NO_2$ is twisted by $\phi_t \approx 75°$ and $-NH_2$ is coplanar with the benzene ring ($\phi_w \approx 0°$). The dependence of H_e on ϕ_t and ϕ_w is shown in Fig. 5c,d. Charge transfer from $-NH_2$ to $-NO_2$ changes the geometries of these groups and their mobilities: $-NO_2$ becomes more located in a plane perpendicularly to the benzene ring while $-NH_2$ now wags around a planar conformation. The relaxed transition energy E_{eg} for stimulated emission (see Fig. 5e) is shown as solid circles while E'_{eg} (open circles) corresponds to the nonrelaxed case. The difference $(E'_{eg} - E_{eg}) \approx 0.4$ eV (3000 cm^{-1}) is essentially the sum of intramolecular reorganization energies in e and g which comes from all degrees of freedom except the $-NO_2$ twisting coordinate. Note also in Fig. 5e that E_{eg} decreases with increasing ϕ_t and turns to zero at $\phi_t \approx 60°$. At this point the excited and ground electronic states are isoenergetic, vibronic coupling therefore become resonant, thus opening channels to internal conversion.

The calculated value $E_{eg} = 2$ eV (620 nm) for the stimulated emission band differs from the experimental one, 520 nm in acetonitrile and 570 nm in water. Better agreement is found for excited-state absorption. Here calculated $E_{en} = 4$ eV (305 nm) compares well with the experimental value of 310 nm. Note that for ESA, the transition energy E_{en} (Fig. 5e) and oscillator strength f_{en} (Fig. 5g) are nearly independent on $-NO_2$ twisting while for SE both E_{eg} and f_{eg} decrease with increasing ϕ_t. As concerns the wagging angle ϕ_w, both $E_{eg}(\phi_w)$ and $f_{eg}(\phi_w)$ equal zero for the relaxed excited-state geometry with $\phi_t = 75°$. Therefore these quantities are shown only for nonrelaxed case in Fig. 5f,h.

6. Interpretation of the spectral evolution before 1 ps

With the results from the previous two sections the early spectral evolution can be treated as follows. Femtosecond optical excitation of PNA results in a nonequilibrium excited state which relaxes in several stages. The fastest process develops on a 10 fs time scale and corresponds to intramolecular vibrational relaxation of high frequency modes [26,32,33]. This process is not resolved in our transient spectra but may be behind an initial red shift of the SE band (peaked at 440 nm for acetonitrile) from the excitation wavelength at 400 nm (Fig. 2a). This shift of 2300 cm^{-1} agrees reasonably with the calculated reorganization energy for coordinates other than $-NO_2$ twisting, $(E'_{eg} - E_{eg}) \approx 3000$ cm^{-1}.

The next process, on a 100 fs time scale, corresponds to solvation and is seen as the dynamic Stokes shift of the SE band. We assume that PNA experiences no intramolecular changes during this process. Therefore all spectral features observed in Fig. 2a,c, such as the hump around 540 nm, are assigned to excited-state absorption. Our calculations indeed predict an ESA band at 2 eV (620 nm, E_{em} in Fig. 5f) with a small oscillator strength $f_{em} = 0.05$ (Fig. 5h).

Intramolecular charge transfer and internal conversion are accessed by twisting of $-NO_2$ when it is driven to a new equilibrium around $\phi_t = 75°$. This happens roughly between 100 fs and 1 ps (Fig. 2b,d) and is recognized by the simultaneous decay of the ESA and SE band. In fact, the decay times for ESA and SE are different. The difference in the two decays is especially pronounced when comparing the transient spectra at 100 and 200 fs (Fig. 2b,d). During this time interval, a small change in excited-state absorption is accompanied by considerable decay of stimulated emission. Numerically the decay times in water are 250 fs for ESA and 120 fs for SE. In acetonitrile the difference is even larger: 400 and 140 fs. This difference allows the distinction of two processes: twisting of $-NO_2$ connected to intramolecular CT, and internal conversion. As follows

from Fig. 5g, the oscillator strength f_{en} for ESA is nearly independent on ϕ_t while f_{eg} for SE rapidly decreases with increasing ϕ_t. Therefore the experimentally observed decay of the ESA band can be directly related to depopulation of the excited state due to internal conversion. For stimulated emission, the decay must be faster because the decrease of f_{eg} (Fig. 5g) gives an additional contribution. Thus the decay of SE characterizes the twisting process while the decay of ESA reflects the internal conversion.

An estimate for the time τ_t of $-NO_2$ twisting may be obtained from the calculated dependence $H_e(\phi_t)$ in Fig. 5c. Neglecting friction, one can write

$$J\frac{d^2\theta_t}{dt^2} = M$$

where $J = 6 \times 10^{-39}$ g cm^2 is the moment of inertia of $-NO_2$, and M is the torque which is taken as constant in the range $30° < \phi_t < 70°$. Then with $M = (H_e(30°) - H_e(70°))/40° = 10^{-12}$ g cm^2 s^{-2} one obtains $\tau_t = 100$ fs. This is in good agreement with the measured relaxation time of stimulated emission in both liquids.

Interestingly, the essential features of the spectral evolution discussed above are reflected in the behavior of the full band integral (dashed line) in Fig. 4a. Here a fast initial decay between 100 and 200 fs (region I, see insert) corresponds to $-NO_2$ twisting. It is followed by a slower decay with $\tau_{ic} \approx 200$ fs (region II) which corresponds to internal conversion. After 1 ps (region III), the full band integral is close to zero. This region will be discussed in the next section.

7. Cooling

The spectral evolution from 1 to 10 ps has been already assigned to cooling of hot PNA molecules in the ground state by the solvent. One argument for this assignment is that reconstructed ground-state spectra in Fig. 3b look like expected hot absorption spectra – they are broadened and shifted to the red. Additionally, our semiempirical calculations do not predict absorbing states with a significant oscillator strength after $-NO_2$ twisting.

Nevertheless imagine for a moment that photo-excited PNA molecule relaxes to an intermediate electronic state. Then the spectral evolution in Fig. 3a can be treated as internal conversion from this intermediate to the ground state, an exponential decay being expected for the band peaked at 450 nm. We have checked this assumption by calculating the associated band integral (from 430 to 709 nm) which characterizes the decay of the band. The behavior of this band integral is shown in Fig. 4b on a logarithmic scale and is clearly non-exponential. Another argument against an intermediate state comes from the evolution of the full band integral. As was already mentioned, this integral reaches zero at a relatively early time of 1 ps (Fig. 4a) although the spectral evolution is by no means finished. Therefore the oscillator strengths for transitions emanating from the intermediate are required to balance those for the ground state – which is unlikely. On the other hand the condition that the band integral vanishes follows directly from the 'hot absorption' hypothesis. Heating of a molecule broadens its absorption spectrum and shifts it to the red but does not change, to a first approximation, the oscillator strength. Therefore the band integral calculated for the sum of this hot spectrum and of corresponding bleach *must* be zero. We would like to stress this criteria: turning the full band integral to zero can be considered as a strong indication of hot ground-state absorption. On this basis we conclude that the spectral evolution between 1 and 10 ps does reflect the cooling of PNA molecules.

We now try to describe the cooling process quantitatively. For this we use the band integral discussed above, for the spectral range 430–709 nm. As seen from Fig. 3, this region most prominently reflects changes in the molecular temperature T. We further assume that the red shift and broadening of the hot spectra depend *linearly* on T. Then the band integral shown in Fig. 4b will be proportional to the temperature of PNA molecules. Linear dependence of the absorption coefficient on molecular temperature was found, for example, for azulene in solution over a range of frequencies in the red wing of the absorption spectrum [20]. To determine the absolute value of T, we measured the stationary absorption spectrum of PNA in water at 90°C and compared it to the transient spectra in Fig. 3b. Good correspondence

was found for the spectrum at 4 ps. With $T = 360$ K at 4 ps, the dependence in Fig. 4b results in a temperature of 800 ÷ 900 K at 1 ps. The temperature at earlier time is estimated from the energy δE deposited to the ground state. It can be expressed as

$$\delta E = hc \cdot (\nu_{ex} - \Delta\nu_{solv}) \quad (6)$$

here $\nu_{ex} = 25\,000$ cm^{-1} is the excitation frequency, and $\Delta\nu_{solv} = 4000$ cm^{-1} for water is the energy transferred directly to the solvent. With the heat capacity of PNA molecule from the calculated vibrational spectrum, Eq. (6) gives for the initial temperature $T_0 = 1400 \pm 50$ K.

The cooling dynamics, as is reflected by the behavior of the band integral in Fig. 4b, may be characterized by two kinds of fitting. At early time between 1 and 3 ps, the decay is exponential (dashed line in Fig. 4b) with a characteristic time of 1.3 ps. At longer delays, after 3 ps, the behavior is clearly nonexponential, instead it satisfies a power dependence $[(t - t_0)/\tau]^{-3/2}$ (solid line) with $t_0 = 0.8$ ps and $\tau = 0.85$ ps. Interestingly this dependence is predicted by the Fourier heat conductivity equation for a point and instantaneous source of heat [34]. The applicability of the Fourier equation will not be discussed in this Letter. Here we only point out that the observed heat transfer is extremely fast, a characteristic time being roughly of 1 ps. This is one order of magnitude faster than, for example, cooling of azulene in acetonitrile [20]. A major reason for such a difference lies to our opinion in very different solute–solvent coupling [35]. Azulene is practically nonpolar and therefore interacts weakly with a bath. In contrast PNA is highly polar, its interaction with polar environment is much stronger that results in the observed acceleration of the cooling process.

8. Conclusion

We summarize briefly the results of this Letter. PNA in polar solutions was studied experimentally, by stationary and transient absorption spectroscopy, and theoretically with semiempirical calculations. Stationary absorption spectra of PNA are affected by the ground-state molecular geometry, namely they depend on the twisting angle of the $-NO_2$ group and on the wagging angle of the $-NH_2$ group. $-NO_2$ rotates nearly freely in the ground state but it is oriented perpendicularly to the benzene ring in the excited electronic state.

The relaxation of the PNA molecule after photoexcitation is initiated by the twist of $-NO_2$ to a new equilibrium position. We studied this process with broadband transient absorption spectroscopy which allows to observe the complete spectral evolution of the pump–probe signal. The relaxation develops as follows. (i) High frequency vibrational modes of PNA relax on a 10 fs time scale. (ii) Solvation in water and acetonitrile is finished before 100 fs. (iii) $-NO_2$ experiences twisting with 120 fs in water and with 140 fs in acetonitrile. (iv) Internal conversion initiated by $-NO_2$ twisting occurs with a time constant of 250 fs in water and of 400 fs in acetonitrile. (v) The hot ground state created by internal conversion cools down with ca. 1 ps both in water and acetonitrile.

Acknowledgements

We thank Heidi Steingraber for steady-state measurements. The Deutsche Forschungsgemeinschaft is gratefully acknowledged for financial support through the Leibniz program.

References

[1] O.S. Khalil, C.J. Seliskar, S.P. McGlynn, J. Chem. Phys. 58 (1973) 1607.
[2] S. Millefiori, G. Favini, A. Millefiori, D. Grasso, Spectrochim. Acta 33 (1975) 21.
[3] T.P. Carsey, G.L. Findley, S.P. McGlynn, JACS 101 (16) (1979) 4502.
[4] J.N. Woodford, M.A. Pauley, C.H. Wang, J. Phys. Chem. A 101 (1997) 1989.
[5] S.P. Karna, P.N. Prasad, M. Dupuis, J. Chem. Phys. 94 (1991) 1171.
[6] B. Champagne, Chem. Phys. Lett. 261 (1996) 57.
[7] J.L. Bredas, F. Meyers, Nonlinear Opt. 1 (1991) 119.
[8] H.K. Sinha, K. Yates, Can. J. Chem. 69 (1990) 550.
[9] W. Schuddeboom, J.M. Warman, H.A.M. Biemans, E.W. Meijer, J. Phys. Chem. 100 (1996) 12369.
[10] C.L. Thomsen, J. Thøgersen, S.R. Keiding, J. Phys. Chem. A 102 (1998) 1062.
[11] M. Godfrey, J.N. Murrell, Proc. R. Soc. A 278 (1964) 71.
[12] R.W. Bigelow, H.-J. Freund, B. Dick, Theor. Chim. Acta 63 (1983) 177.

[13] P.C. Hiberty, G. Ohanessian, JACS 106 (1984) 6963.
[14] J.O. Morley, J. Phys. Chem. 98 (1994) 13182.
[15] J. Czekalla, G. Wick, Z. Electrochem. 65 (1961) 727.
[16] S.A. Kovalenko, A.L. Dobryakov, J. Ruthmann, N.P. Ernsting, Phys. Rev. A 59 (1999) 2369.
[17] S.A. Kovalenko, N.P. Ernsting, J. Ruthmann, Chem. Phys. Lett. 258 (1996) 445.
[18] U. Sukowski, A. Seilmeier, T. Elsaesser, S.F. Fischer, J. Chem. Phys. 93 (1990) 4094.
[19] R.J. Sension, S.T. Repinec, A.Z. Szarka, R.M. Hochstrasser, J. Chem. Phys. 98 (1993) 6291.
[20] D. Schwarzer, J. Troe, M. Votsmeier, M. Zerezke, J. Chem. Phys. 105 (1996) 3121.
[21] D. Schwarzer, J. Troe, M. Zerezke, J. Chem. Phys. 107 (1997) 8380.
[22] C. Heidelbach, I.I. Fedchenia, D. Schwarzer, J. Schroeder, J. Chem. Phys. 108 (1998) 10152.
[23] S. Sartania, Z. Cheng, M. Lenzner, G. Tempea, Ch. Spielmann, F. Krausz, K. Ferencz, Opt. Lett. 22 (1997) 1562.
[24] N. Mataga, T. Kubota, Molecular Interactions and Electronic Spectra, New York, 1970.
[25] R. Jimenez, G.R. Fleming, P.V. Kumar, M. Maroncelli, Nature 369 (1994) 471.
[26] M.L. Horng, J.A. Gardecki, A. Papazyan, M. Maroncelli, J. Phys. Chem. 99 (1995) 17311.
[27] J. Ruthmann, S.A. Kovalenko, N.P. Ernsting, D. Ouw, J. Chem. Phys. 109 (1998) 5466.
[28] W. Liptay, in: E.C. Lim (Ed.), Excited States, vol. 1, New York, 1974, p. 129.
[29] V.M. Farztdinov, S.A. Kovalenko, N.P. Ernsting, submitted to PCCP.
[30] A. Klamt, J. Phys. Chem. 100 (1996) 3349.
[31] S. Millefiori, G. Favini, D. Grasso, Spectrochim. Acta 33A (1977) 21.
[32] S.A. Kovalenko, J. Ruthmann, N.P. Ernsting, J. Chem. Phys. 109 (1998) 1894.
[33] Handbook of Chemistry and Physics, 79th edn., CRC Press, New York 1998.
[34] L.D. Landau, E.M. Lifshitz, Fluid Mechanics, 2nd edn., New York, 1995.
[35] B.M. Ladanyi, R.M. Stratt, J. Chem. Phys. 111 (1999) 2008.